

Jamming below upper critical dimension

Harukuni Ikeda^{1,*}

¹*Laboratoire de Physique de l'École Normale Supérieure, Université PSL,
CNRS, Sorbonne Université, Université de Paris, 75005 Paris, France*

(Dated: July 17, 2022)

Extensive numerical simulation in the past decades proved that the critical exponents of the jamming of frictionless spherical particles remain unchanged in two and three dimensions. This implies that the upper critical dimension is $d_u = 2$ or lower. In this work, we study the jamming transition below the upper critical dimension. We investigate a quasi-one-dimensional system: disks confined in a narrow channel. We show that the system is isostatic at the jamming transition point as in the case of standard jamming transition of the bulk systems in two and three dimensions. Nevertheless, the scaling of the excess contact number shows the linear scaling. Furthermore, the gap distribution remains finite even at the jamming transition point. These results are qualitatively different from those of the bulk systems in two and three dimensions.

PACS numbers: 64.70.Q-, 05.20.-y, 64.70.Pf

Introduction. – When compressed, particles interacting with finite ranged potential undergo the jamming transition at the critical packing fraction $\varphi = \varphi_J$ at which particles start to touch, and the system acquires rigidity without showing apparent structural changes [1]. One of the most popular models of the jamming transition is a system consisting of frictionless spherical particles [2]. The nature of the jamming transition of the model is now well understood due to experimental and numerical investigations [1]. A few remarkable properties are the following: (i) the system is nearly isostatic at φ_J ; namely, the number of constraints is just one greater than the number of degrees of freedom [3], (ii) the excess contact number δz from the isostatic value exhibits the power-law scaling $\delta z \sim \delta\varphi^a$ where $\delta\varphi = \varphi - \varphi_J$ denotes the excess packing fraction [2], (iii) the distribution of the gap between particles $g(h)$ exhibits the power-law divergence $g(h) \sim h^{-\gamma}$ at φ_J [4], and (iv) the critical exponents, $a = 1/2$ and $\gamma = 0.41$, do not depend on the spatial dimensions d [2, 5].

On the theoretical side, one of the greatest achievements is the exact calculation of the critical exponents by using the mean-field models such as infinite dimensional hard spheres [5] and perceptron [6]. These models can be analyzed by using the notorious replica method, which was originally developed for polymers and spin-glasses [7]. The replica method predicts that systems undergo the replica symmetric breaking (RSB) transition before the jamming transition point [8]. Analyzing the jamming transition in the RSB phase, the replica theory can reproduce the isostaticity at φ_J , and the correct values of the critical exponents a and γ [5, 9]. These results imply that the upper critical dimension d_u , above which the mean-field theory provides correct results, is $d_u \leq 2$. Interestingly, an Imry-Ma-type argument also suggests $d_u = 2$ [10].

A natural question is then what will happen below the upper critical dimension. To answer this question,

we here investigate the jamming transition for $d < 2$. However, the jamming transition of true $d = 1$ system is a rather trivial: rods on the line begin to contact at $\varphi_J = 1$, and for $\varphi \geq \varphi_J$, each particle has two contact $z = 2$ unless next nearest neighbor particles begin to interact at very high φ . To obtain non-trivial results, we consider a quasi-one-dimensional system as shown in Fig. 1, where particles are confined between the walls at $y = 0$ and $y = L_y$, and for x -direction, we impose the periodic boundary condition. In the thermodynamic limit with fixed L_y , the model can be considered as a one-dimensional system, but the jammed configuration is still far from trivial.

In the previous works, quasi-one-dimensional systems have been studied to elucidate the effect of confinement on the jamming transition [11, 12]. These studies uncover how the confinement changes the transition point φ_J [12] and the distribution of the stress near the wall [11]. However, the investigation of the critical properties is limited for the systems with very small L_y where the jammed configuration is similar to that of the true $d = 1$ system: each particle contact with at most two particles, and therefore one can not discuss the scaling of δz [13–15]. To our knowledge, the scaling of δz for an intermediate value of L_y has not been studied before.

By means of extensive numerical simulations, we show that the system is always isostatic at the jamming transition point for all values of L_y , as in the case of the jamming in $d \geq 2$. Nevertheless, the critical behavior of the jamming of the quasi-one-dimensional system is dramatically different from the jamming transition in $d \geq 2$. We find that the excess contact number δz , and the excess constraints δc , which plays a similar role as δz , exhibit the linear scaling $\delta z \sim \delta c \sim \delta\varphi$. Furthermore, we find that $g(h)$ remains finite even at φ_J . These results imply that the jamming of the quasi-one-dimensional system indeed belongs to a different universality class than the jamming in $d \geq 2$.

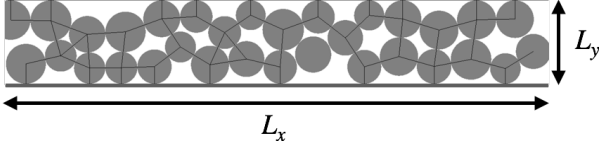


FIG. 1. A configuration at φ_J for $N = 32$ and $L_y = 2\sigma_{\max}$. Gray circles represent particles, and the solid lines denote the contacts.

Model. – Here we describe the details of our model. We consider two dimensional disks in a $L_x \times L_y$ box. For the y -direction, particles are confined between the walls at $y = 0$ and $y = L_y$. For the x -direction, we impose the periodic boundary condition. The interaction potential of the model is given by

$$\begin{aligned}
 V_N &= \sum_{i < j}^{1,N} v(h_{ij}) + \sum_{i=1}^N v(h_i^b) + \sum_{i=1}^N v(h_i^t), \\
 h_{ij} &= |\mathbf{r}_i - \mathbf{r}_j| - \frac{\sigma_i + \sigma_j}{2}, \\
 h_i^b &= y_i - \frac{\sigma_i}{2}, \\
 h_i^t &= L_y - y_i - \frac{\sigma_i}{2}, \\
 v(h) &= k \frac{h^2}{2} \theta(-h).
 \end{aligned} \tag{1}$$

where $\mathbf{r}_i = \{x_i, y_i\}$ and σ_i respectively denote the position and diameter of particle i , h_{ij} denotes the gap function between particles i and j , and h_i^b and h_i^t respectively denote the gap functions between particles i and bottom and top walls. To avoid the crystallization, we consider polydisperse particles with uniform distribution $\sigma_i \in [\sigma_{\min}, \sigma_{\max}]$. Here after we set, $k = 1$, $\sigma_{\min} = 1$, and $\sigma_{\max} = 1.4$.

Numerics. – We perform numerical simulations for $N = 1024$ disks. We find φ_J by combining slow isotropic compression and decompression as follows [2]. We first generate a random initial configuration at a small packing fraction $\varphi = 0.1$ between the walls at $y = 0$ and $y = L_y$. Then, we slowly compress the system by performing an affine transformation along the x -direction. For each compression step, we increase the packing fraction with a small increment $\delta\varphi = 10^{-3}$, and successively minimize the energy with the FIRE algorithm [16] until the squared force acting on each particle becomes smaller than 10^{-25} . After arriving at a jammed configuration with $V_N/N > 10^{-16}$, we change the sign and amplitude of the increment as $\delta\varphi \rightarrow -\delta\varphi/2$. Then, we decompress the system until we obtain an unjammed configuration with $V_N/N < 10^{-16}$. We repeat this process by changing the sign and amplitude of the increment as $\delta\varphi \rightarrow -\delta\varphi/2$ every time the system crosses the jamming transition point. We terminate the simulation when $V_N/N \in (10^{-16}, 2 \times 10^{-16})$. We define φ_J as a packing

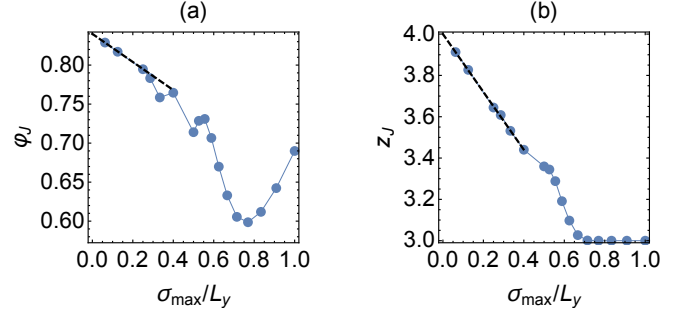


FIG. 2. L_y dependence of (a) the jamming transition point φ_J and (b) the contact number per particle at the jamming transition point z_J . Markers denote numerical results, and solid lines denote the guide to the eye. The dashed lines denote the linear fits $\varphi_J = 0.84 - 0.28\sigma_{\max}/L_y$ and $z_J = 4 - 1.4\sigma_{\max}/L_y$.

fraction of this point.

After obtained a configuration at φ_J , we re-compress the system to obtain configurations above φ_J . As reported in Ref. [17], some fraction of samples become unstable during the compression (compression unjamming). We neglect those samples. We remove the rattlers that have zero or one contact before calculating physical quantities. To improve the statistics, we average over 50 independent samples.

Results. – First, we discuss the L_y dependence of the jamming transition point φ_J and the contact number per particle at that point z_J . In Fig. 2 (a), we show φ_J as a function of σ_{\max}/L_y . For intermediate values of σ_{\max}/L_y , φ_J shows a non-monotonic behavior. Similar non-monotonic behaviors are reported in previous numerical simulations of the jamming of binary mixtures [12]. In the limit $\sigma_{\max}/L_y \rightarrow 0$, φ_J converges to its bulk value $\varphi_J^{\text{bulk}} = 0.84$ as $\varphi_J^{\text{bulk}} - \varphi_J \propto 1/L_y$, see the dashed line in Fig. 2 (a). The same scaling was also observed in the previous simulations for binary mixtures [12]. The scaling implies the growing length scale

$$\xi \sim (\varphi_J^{\text{bulk}} - \varphi)^{-\nu} \tag{2}$$

with $\nu = 1$. It is worth mentioning that this is the same exponent observed by the correction to scaling analysis [18] and also our replica calculation for a confined system [19].

In Fig. 2 (b), we show z_J as a function of σ_{\max}/L_y . It is well known that $z_J = z_J^{\text{bulk}} = 4$ for bulk two dimensional disks [2]. In the $L_y \rightarrow \infty$ limit, z_J converges to the bulk value as $z_J^{\text{bulk}} - z_J \sim 1/L_y$, see the dashed line in Fig. 2 (b).

Next we discuss the isostaticity of the system. A system is referred to as isostatic when the number of constraints is the same as the number of degrees of freedom. For our system, the number of degrees of freedom

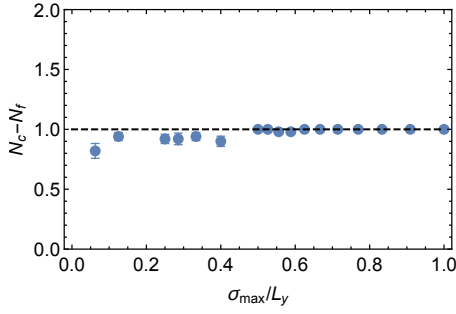


FIG. 3. L_y dependence of $N_c - N_f$.

is $N_f = 2N - 1$ where we neglect the global translation along the x -axis. The number of constraints is

$$N_c = \frac{Nz - N_w}{2} + N_w = \frac{Nz}{2} + \frac{N_w}{2}, \quad (3)$$

where z denotes the number of contacts per particles, N_w denotes the number of contacts between particles and walls, and $(Nz - N_w)/2$ accounts for the number of contacts between particles. When $L_y \gg \sigma_{\max}$, the number of contacts between particles and walls can be negligible, $Nz/2 \gg N_w$, and the isostatic condition $N_c = N_f$ leads to $z = 4$ in the thermodynamic limit. This condition is indeed satisfied in the case of the bulk $d = 2$ system at φ_J [2]. More strictly, a bulk system at φ_J in $d \geq 2$ satisfies $N_c \approx N_f + 1$, which is the minimal number of constraints to stabilize the system [20]. On the contrary for $L_y \sim \sigma_{\max}$, all particles may contact with walls $N_w = N$, leading to $z = 3$ for an isostatic system. Fig. 2 (b) show that our model satisfies this condition at φ_J for small L_y . To investigate the isostaticity for finite L_y , in Fig. 3, we plot $N_c - N_f$ at φ_J as a function of σ_{\max}/L_y . The plot proves that the system satisfies $N_c \approx N_f + 1$, irrespective of the value of L_y , as in the case of the bulk systems in $d \geq 2$ [20].

Now we shall discuss the behavior above φ_J . For $\varphi > \varphi_J$, the particles overlap each other. As a consequence, the energy V_N and pressure p have finite values. Since we only consider the compression along the x -axis in this work, we define the pressure as

$$p = -\frac{1}{V} \left. \frac{\partial V_N(\{x'_i\})}{\partial \varepsilon} \right|_{\varepsilon=0} = -\frac{1}{V} \sum_{i < j} v'(h_{ij}) \frac{(x_i - x_j)^2}{|\mathbf{x}_i - \mathbf{x}_j|}, \quad (4)$$

where $V = L_x L_y$, and $x'_i = x_i(1 + \varepsilon)$ denotes the affine transformation along the x -axis. In Fig. 4, we show the $\delta\varphi$ dependence of V_N/N and p . We find the scalings $V_N/N \sim \delta\varphi^2$ and $p \sim \delta\varphi$. The same scalings were observed for the bulk systems in $d = 2$ and $d = 3$ [2].

Next we observe how the number of the excess constraints increases on the compression. We define the ex-

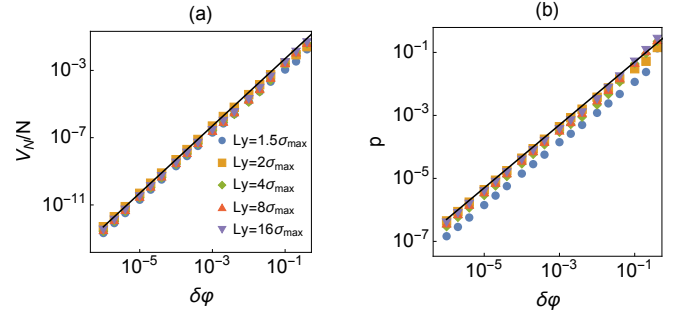


FIG. 4. (a) $\delta\varphi$ dependence of the energy per particle V_N/N . Marker denote numerical results, and the solid line denotes $\delta\varphi^2$. (b) $\delta\varphi$ dependence of the pressure p . Marker denote numerical results, and the solid line denotes $\delta\varphi$.

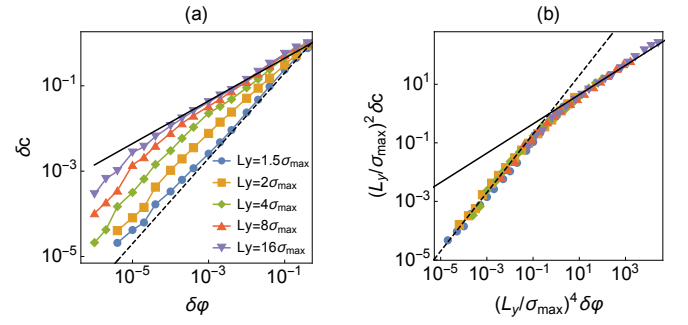


FIG. 5. (a) δc as a function of $\delta\varphi$. Markers denote numerical results. The solid and dashed lines denote $\delta c \sim \delta\varphi^{1/2}$ and $\delta c \sim \delta\varphi$, respectively. (b) Scaling plot for the same data.

cess constraints per particle as

$$\delta c = \frac{N_c - N_f - 1}{N}. \quad (5)$$

When $L_y \gg \sigma_{\max}$, δc converges to $\delta z/2$, and is supposed to show the same scaling as the bulk systems $\delta c \sim \delta\varphi^{1/2}$ [2]. Here we want to investigate how the behavior changes for finite L_y . In Fig. 5 (a), we show the $\delta\varphi$ dependence of δc for several L_y . For $L_y \gg \sigma_{\max}$, δc develops the intermediate regime where one observes the square root scaling $\delta c \sim \delta\varphi^{1/2}$. On the contrary, for small L_y , δc develops the linear behavior $\delta c \sim \delta\varphi$. To discuss how the crossover takes place from the large L_y to small L_y behaviors, we assume the following scaling form:

$$\delta c = l_y^\alpha \mathcal{C}(l_y^\beta \delta\varphi), \quad (6)$$

where $l_y = L_y/\sigma_{\max}$, and the scaling function $\mathcal{C}(x)$ behaves as

$$\mathcal{C}(x) \sim \begin{cases} x^{1/2} & x \gg 1 \\ x & x \ll 1. \end{cases} \quad (7)$$

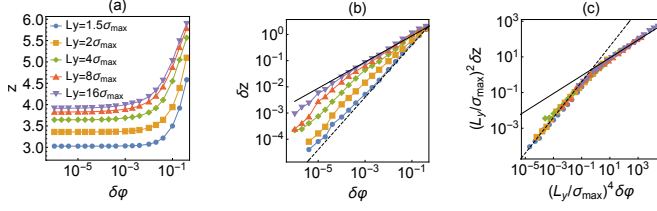


FIG. 6. (a) z as a function of $\delta\varphi$. Markers denote numerical results. (b) $\delta z = z - z_J$ as a function of $\delta\varphi$. The solid and dashed lines denote $\delta z \sim \delta\varphi^{1/2}$ and $\delta z \sim \delta\varphi$, respectively. (c) Scaling plot for the same data.

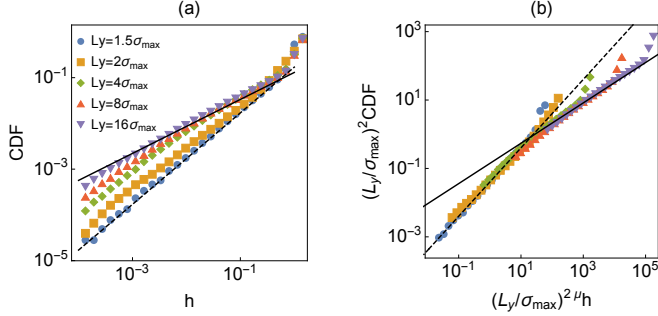


FIG. 7. (a) CDF of the gap function h . Markers denote numerical results. The solid and dashed lines denote $h^{1-\gamma}$ and h^1 , respectively. (b) Scaling plot for the same data.

When $l_y \sim \sqrt{N}$, the scaling should converge to that of the bulk $d = 2$ system. Far from the transition point, we have $\delta c \sim \delta z \sim \delta\varphi^{1/2}$, which requires $\alpha + \beta/2 = 0$. Contrary, the behavior near the transition point should be $\delta c \sim N\delta\varphi$ [20], which requires $\alpha + \beta = 2$. Therefore, we have $\alpha = -2$ and $\beta = 4$. In Fig. 5, we test this prediction. A good scaling collapse verifies the scaling function Eq. (6).

In Figs.(a)–(c), we also show the behaviors of the contact number per particle z , excess contacts $\delta z = z - z_J$, and its scaling plot. The data for δz is more noisy than δc , presumably due to the fluctuation of z_J , but still we find a reasonable scaling collapse by using the same scaling form of δc .

Another important quantity to characterize the critical property of the jamming transition is the gap distribution $g(h)$. For the bulk systems in $d \geq 2$, $g(h)$ exhibits the power-law divergence at φ_J :

$$g(h) \sim h^{-\gamma} \quad (8)$$

with $\gamma = 0.41$ [5]. In order to improve the statistics, we observe the cumulative distribution function (CDF) of the gap functions (h_{ij} and $h_i^{t,b}$), instead of $g(h)$ itself. In this case, the power-law divergence Eq. (8) appears as $\text{CDF} \sim h^{1-\gamma}$. In Fig. 7 (a), we show our numerical results of CDF for several L_y . We find that for small L_y and h ,

$\text{CDF} \sim h$ meaning that $g(h)$ remains finite $g(h) \sim h^0$ even at φ_J . On the contrary, for large L_y , there appears the intermediate regime where $\text{CDF} \sim h^{1-\gamma}$, as in $d \geq 2$. To discuss the crossover from $\text{CDF} \sim h$ to $\text{CDF} \sim h^{1-\gamma}$, we assume the following scaling form:

$$\text{CDF} = l_y^{\alpha'} \mathcal{F}(l_y^{\beta'} h), \quad (9)$$

where the scaling function $\mathcal{F}(x)$ behaves as

$$\mathcal{F}(x) \sim \begin{cases} x^{1-\gamma} & x \gg 1 \\ x & x \ll 1. \end{cases} \quad (10)$$

When $l_y \sim \sqrt{N}$, this should converge to the scaling form for finite N , $\text{CDF}(h) = N^{-1} \mathcal{F}(N^\mu h)$, where $\mu = 1/(1 - \gamma)$ [21]. This requires $\alpha' = -2$ and $\beta' = 2\mu$. In Fig. 7 (b), we check this prediction. The excellent collapse proves the validity of our scaling Ansatz Eq. (9).

Conclusions. – In this work, we showed that the jamming transition in a quasi-one-dimensional system is qualitatively different from that of the $d \geq 2$ systems: the excess constraints and contacts exhibit the linear scaling $\delta c \sim \delta z \sim \delta\varphi$ instead of the square root scaling observed in $d \geq 2$, and the gap distribution $g(h)$ remains finite even at φ_J . This implies that the universality class of the jamming of the quasi-one-dimensional system is different from that of the $d \geq 2$ systems.

Important future work is to test the robustness of our results for other shapes of the quasi-one-dimensional geometries such as a d -dimensional box with a fixed length in the $d - 1$ directions and an infinite length in only one direction, and circular cylinder with a fixed radius.

Interestingly, the same scaling behavior of that of our model has been reported for a model of random linear programming [6], where the system becomes isostatic at the jamming transition point, but the RSB does not happen. As a consequence, $g(h)$ remains finite and regular. Considering this result, our results may imply that the RSB phase does not appear even at φ_J in $d = 1$, while it does in $d = 2$, namely, the lower critical dimension of the RSB at φ_J is $1 < d_l < 2$. Further theoretical investigations are necessary to elucidate this point.

Acknowledgements. – We warmly thank M. Ozawa, A. Ikeda, K. Hukushima, Y. Nishikawa, F. Zamponi, and P. Urbani for discussions related to this work. This project has received funding from the European Research Council (ERC) under the European Union's Horizon 2020 research and innovation program (grant agreement n. 723955-GlassUniversality).

* harukuni.ikeda@ens.fr

[1] A. J. Liu and S. R. Nagel, Annu. Rev. Condens. Matter Phys. 1, 347 (2010).

- [2] C. S. O'Hern, L. E. Silbert, A. J. Liu, and S. R. Nagel, Phys. Rev. E **68**, 011306 (2003).
- [3] J. Bernal and J. Mason, Nature **188**, 910 (1960).
- [4] A. Donev, S. Torquato, and F. H. Stillinger, Phys. Rev. E **71**, 011105 (2005).
- [5] P. Charbonneau, J. Kurchan, G. Parisi, P. Urbani, and F. Zamponi, Nat. Commun. **5**, 3725 (2014).
- [6] S. Franz and G. Parisi, Journal of Physics A: Mathematical and Theoretical **49**, 145001 (2016).
- [7] M. Mézard, G. Parisi, and M. Virasoro, *Spin glass theory and beyond: An Introduction to the Replica Method and Its Applications*, Vol. 9 (World Scientific Publishing Company, 1987).
- [8] J. Kurchan, G. Parisi, P. Urbani, and F. Zamponi, The Journal of Physical Chemistry B **117**, 12979 (2013).
- [9] S. Franz, G. Parisi, M. Sevelev, P. Urbani, and F. Zamponi, SciPost Phys **2**, 019 (2017).
- [10] M. Wyart, arXiv preprint cond-mat/0512155 (2005).
- [11] J. W. Landry, G. S. Grest, L. E. Silbert, and S. J. Plimpton, Physical review E **67**, 041303 (2003).
- [12] K. W. Desmond and E. R. Weeks, Phys. Rev. E **80**, 051305 (2009).
- [13] S. S. Ashwin and R. K. Bowles, Phys. Rev. Lett. **102**, 235701 (2009).
- [14] S. S. Ashwin, M. Zaeifi Yamchi, and R. K. Bowles, Phys. Rev. Lett. **110**, 145701 (2013).
- [15] M. J. Godfrey and M. A. Moore, Phys. Rev. E **89**, 032111 (2014).
- [16] E. Bitzek, P. Koskinen, F. Gähler, M. Moseler, and P. Gumbsch, Phys. Rev. Lett. **97**, 170201 (2006).
- [17] K. VanderWerf, A. Boromand, M. D. Shattuck, and C. S. O'Hern, Phys. Rev. Lett. **124**, 038004 (2020).
- [18] D. Vågberg, D. Valdez-Balderas, M. A. Moore, P. Olsson, and S. Teitel, Phys. Rev. E **83**, 030303 (2011).
- [19] H. Ikeda and A. Ikeda, EPL (Europhysics Letters) **111**, 40007 (2015).
- [20] C. P. Goodrich, A. J. Liu, and S. R. Nagel, Physical review letters **109**, 095704 (2012).
- [21] H. Ikeda, C. Brito, and M. Wyart, arXiv preprint arXiv:1908.02091 (2019).